Laser Ultrasonics for Noncontact Measurement of Lamb Waves in Static and Moving Paper

J.H. JONG, P.H. BRODEUR, E.F. LAFOND, J.P. GERHARDSTEIN and B.M. PUFAHL

The experimental demonstration of noncontact laser ultrasonics to monitor Lamb waves and the relevant mechanical behaviour of paper is presented. Measurements were performed in a controlled environment using a variable-speed web simulator. Signals obtained using the photorefractive method on nonmoving paper are discussed and the preliminary analysis of S_0 and A_0 modes is presented. On moving paper, the detection of ultrasonic signals based on the Photo-EMF interferometer technology is reported at production speeds on copy paper and 42 lb linerboard. Preliminary results verify the potential of laser ultrasonics for real-time monitoring of elastic stiffness, bending stiffness and shear rigidity.

Nous faisons ici la démonstration d'essais d'ultrasons laser sans contact pour suivre les ondes Lamb et le comportement mécanique afférent du papier. Les mesures ont été effectuées dans un environnement contrôlé à l'aide d'un simulateur de feuille en continu à vitesse variable. Les signaux obtenus à l'aide de la méthode photoréfractive sur du papier immobile sont discutés et l'analyse préliminaire des modes S_0 et A_0 est présentée. Sur le papier en mouvement, la détection des signaux ultrasoniques basés sur la technologie de l'interféromètre Photo-EMF est reportée à des vitesses de production sur du papier pour reproduction et du carton couverture 42 lb. Les résultats préliminaires confirment le potentiel des ultrasons laser pour le suivi en temps réel de la rigidité élastique, de la rigidité à la flexion et de la rigidité au cisaillement.

INTRODUCTION

The development of on-machine paper stiffness or "strength" sensors has been an on-going process for over 25 years because mechanical properties are critical to the papermaking process, converting operations, and end-use performance [1]. While the development of contact methods is at centre stage [2–16], noncontact methods did not receive full attention even though they are far more desirable to the papermaker [17–21]. Merits of the latter methods include eliminating potential damage to the moving web and monitoring of fine papers, coated grades and paperboards. These same methods may prove beneficial in tissue and wet-end testing. It is expected that the availability of a noncontact method would simplify the development of full-sheet inspection systems for paper stiffness. Assuming that Lamb waves can be excited and detected in a noncontact manner using ultrasonic principles, one distinguishes two different test approaches: air-coupled transduction and laser ultrasonics.

J.H. Jong, P.H. Brodeur*, E.F. Lafond, J.P. Gerhardstein** and B.M. Pufahl
IPST
500 10th St. NW
Atlanta, GA, USA
30318
* Now with:
SoniSys LLS
1734 Cooper Lake Dr.
Smyrna, GA, USA
30080
** Now with :
DAQTRON Inc.
1007-B Mansell Rd.
Roswell, GA, USA
30076

Air-Coupled Transduction

Considerable progress has been made in recent years toward the development of efficient air-coupled capacitive transducers, which are more sensitive and have a larger bandwidth than air-coupled piezoelectric transducers [22]. These transducers are relatively inexpensive. However, their utilization remains limited by the air medium itself: sound absorption in air increases with frequency, sound velocity in air is temperature-dependent, and path lengths are sensitive to turbulence [23]. A resonance technique to induce and detect Lamb waves using air-coupled transducers was successfully tested on nonmoving paperboards [17,18]; an on-line implementation is hardly possible because the transmitter–receiver assembly must be rotated to get the maximum transfer of energy into the paper. Also, since the sheet must be fairly thick to excite Lamb waves (>400 μm), testing of fine paper grades is difficult [18].

Laser Ultrasonics

The second approach, laser ultrasonics, considers the laser generation and detection of Lamb waves. The discipline is now well established [24], and applications

exist in the metal and plastic industries. Merits include point source excitation (ideal configuration for detection of stiffness orientation distribution), absence of measurement artifacts due to the coupling medium (insensitivity to air temperature and moisture, turbulence), uniqueness of information, and large bandwidth. Also, it offers unique conditions for the simultaneous optical detection of fibre orientation distribution using a light-scattering method. Difficulties still exist in relation to surface roughness dependency (speckle averaging), sheet fluttering (also true for air-coupled transduction), and complexity of equipment. There are currently three patents describing the use of lasers to generate Lamb waves in paper [19-21]. However, contact transducers [19,20] and unproved optical deflectometry [21] were used for the detection of Lamb waves. None of these patents considers optical heterodyne interferometry for detection to enhance measurement sensitivity [25]. A formal demonstration of noncontact laser ultrasonics on static paper has been performed [26,27]. Also, a fundamental study of Lamb wave propagation in copy paper using noncontact laser generation and detection principles was investigated [28,29].

The concept of noncontact laser generation and detection of Lamb waves is described schematically in Fig. 1. A high-power pulsed laser beam is focused onto the surface of paper. Upon interaction of laser light with paper, a thermoelastic effect occurs, thus exciting a spectrum of Lamb waves (also called plate waves) in all directions in the plane of paper. An interferometer using a continuous wave (CW) laser is used for ultrasound detection, but a pulsed laser with sufficient coherent length could also be used. Depending upon the position of the detection point with respect to the generation point, waves propagating along machine direction (MD), cross-machine direction (CD), or any other planar directions are detected. Also, two different propagation modes are detected: dilatational and bending modes. Fundamental (zeroth order) dilatational or symmetric (S_0) and bending or antisymmetric (A_0) Lamb wave modes are depicted in Fig. 2.

In this work, results gathered using two promising laser detection systems for paper testing are described: a two-wave mixing photorefractive interferometer (TWM) applied to nonmoving paper and a photo-induced electromotive force (Photo-EMF) interferometer applied to moving paper. Lamb waves were excited using a Q-switched Nd:YAG laser operating at 1064 nm (near infrared). Pulse width and maximum pulse energy were 5–7 ns and a few tens of mJ, respectively. The beam diameter on the paper was less than 1 mm. Under these generating conditions, an intermediate excitation regime between thermoelastic and ablation regime was observed. Additional work beyond the scope of this study is underway to optimize Lamb wave excitation, while preventing any visible damage to paper through ablation.

A schematic diagram of the photorefractive interferometer setup for nonmoving paper testing is shown in Fig. 3. A detailed description of this setup was reported by Lafond et al. [30]. In brief, output from the CW Ar:ion detection laser (λ = 515 nm) is split into two beams: the sample and pump beams. A microscope objective lens is used to focus the sample beam onto the paper surface. The scattered beam carrying the ultrasonic signal is collected by the objective lens and recombined with the pump beam in the $Bi_{12}SiO_{20}$ (BSO) photorefractive crystal. This arrangement is sensitive to nanometre-scale displacements at the surface of paper. The interference signal is detected by a photodiode. The BSO crystal is very sensitive to displacements, but its slow response time (>10 ms) makes it unsuitable for moving paper. A crystal with a faster response time such as gallium arsenide (GaAs) would be more appropriate for a moving surface. One should note in Fig. 3 that the paper surface is at an angle with respect to the optical detection path to optimize the detection of particle motion (Lamb waves) in the plane of paper. The paper sample can be rotated by 90° to perform either MD or CD measurements.

A schematic diagram of the Photo-EMF interferometer for moving paper experiments is shown in Fig. 4. The paper sample is mounted on a computer-controlled, variable-speed, rotating drum capable of simulating web speeds up to 2850 m/min. The presence of a backing material for demonstration purposes does not affect Lamb wave propagation. Details of this setup are presented elsewhere [31]. The detection method is based on the photo-electromotive property of a photorefractive crystal. A small current is created at the surface of the crystal by the slight phase shift of the speckles caused by Lamb wave-induced motion

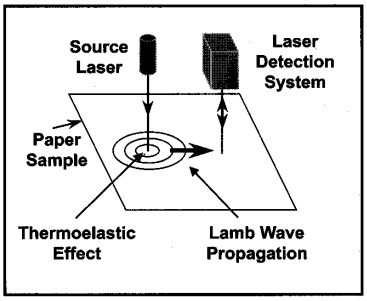

Fig. 1. Laser ultrasonics principles.

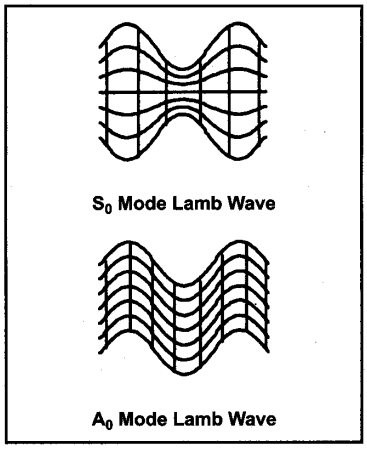

Fig. 2. Cross-sectional view of paper exhibiting the fundamental S_0 and A_0 modes for Lamb waves.

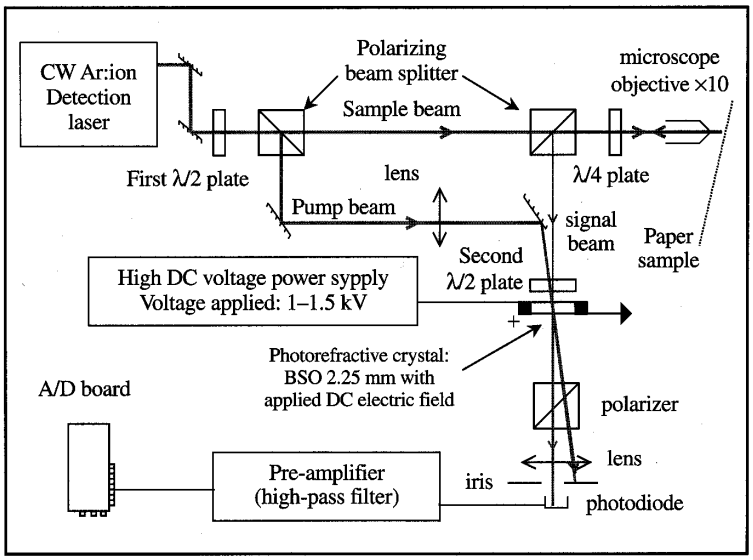

Fig. 3. Schematic diagram of the photorefractive interferometer setup [30].

of the paper surface. The current is picked up by two electrodes located on the sides of the crystal. The frequency response of the Photo-EMF interferometer is relatively flat and very well adapted to Lamb wave detection under continuously changing speckle conditions (moving paper). Moreover, it cuts off low-frequency vibrations, which could be problematic in a mill environment (below 10 kHz).

LAMB WAVE PROPAGATION

Assuming that paper can be modelled as an orthotropic material, i.e. a material that has three mutually orthogonal symmetry planes, relationships exist between paper stiffness properties and different Lamb wave propagation modes [1,18]. For orthotropic symmetry, there are nine independent bulk stiffness coefficients: C_{11}, C_{22}, C_{33}, C_{12}, C_{13}, C_{23}, C_{44}, C_{55} and C_{66} [18,27]. Although bulk stiffnesses are common in expressing 3D linear elasticity, it is convenient to use four planar stiffnesses for Lamb wave propagation in paper: Q_{11}, Q_{22}, Q_{12} and Q_{66}. Strictly speaking, $Q_{11} = C_{11} - C_{13}^2/C_{33}$ and $Q_{22} = C_{22} - C_{23}^2/C_{33}$, but the error is very small and one can assume in practice that $Q_{11} \sim C_{11}$ and $Q_{22} \sim C_{22}$ [27].

Figure 5 illustrates the dispersion behaviour of Lamb waves for the special case of copy paper along machine direction. The dispersion equation [18,32] was solved from the stiffness data gathered using the contact ultrasonic test equipment available at IPST [33,34]. We are concerned mainly with the fundamental S_0 and A_0 modes here. Since the S_0 mode is nondispersive at low frequency (up to the cut-off frequency), a cross-correlation technique can be used to evaluate the wave velocity, from which Q_{11} and Q_{22} are determined (apparent density of paper multiplied by square of velocity) [13].

The A_0 mode relates to both longitudinal and shear stiffness properties. This

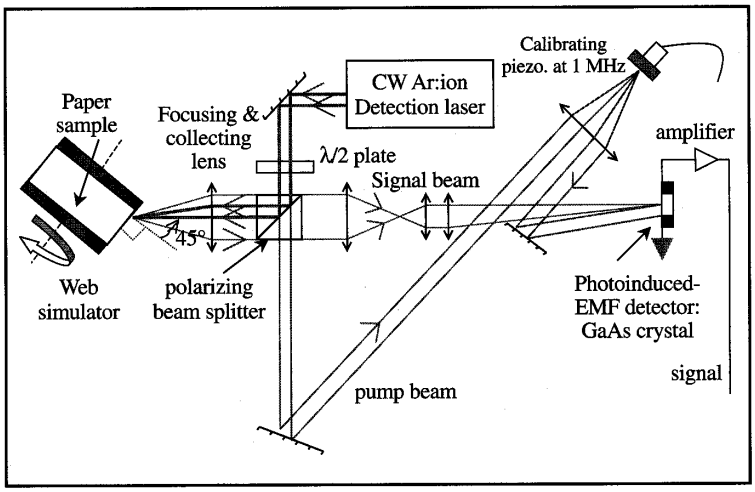

Fig. 4. Schematic diagram of the Photo-EMF interferometer [31]. The variable speed moving web simulator is shown at left.

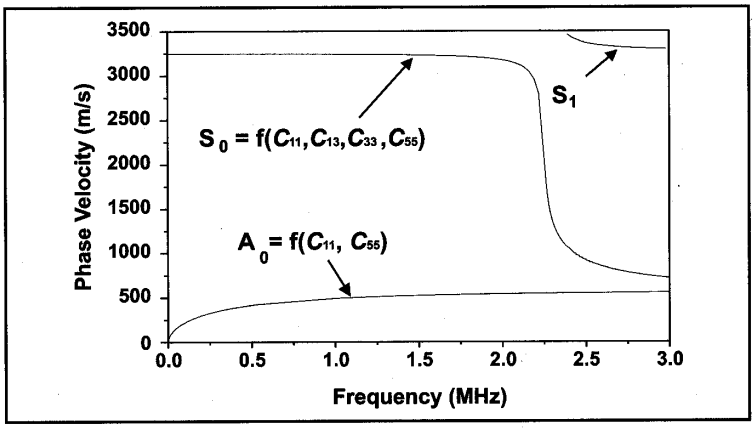

Fig. 5. Typical calculated dispersion curves in MD for copy paper.

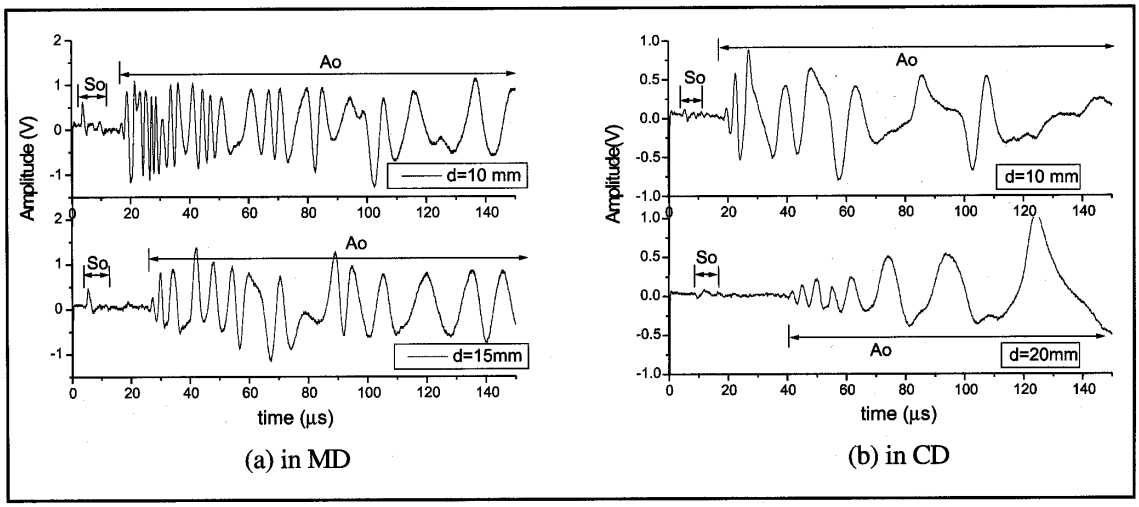

Fig. 6. Single-shot signals collected with the TWM setup for nonmoving copy paper in MD and CD.

mode is dispersive (frequency dependent velocity) at low frequency and reaches a plateau at high frequency [32]. The asymptotic velocity at high frequency is known to be that of a Rayleigh wave, which exists on the surface of a half-space material. It can be used to determine the out-of-plane shear stiff- nesses in MD-ZD and CD-ZD plane directions (C_{55} and C_{44}). As further described below, the phase unwrapping technique developed by Schumacher et al. [35] was used in this work to extract stiffness information from the A_0 mode.

Other important characteristics of the dispersion curves are found by varying the values of the elastic stiffnesses as defined in Ref. [1]. By raising or lowering the value of Q_{11}, one can determine its effect on the S_0 and A_0 modes. The major effect of Q_{11} is on the low-frequency limit of the S_0 mode, while only a minor change is observed in the initial slope of the A_0 mode. The main effect of C_{33} is on the cut-off frequency for the S_0 mode. C_{13} has only a minor effect on the S_0 mode. The effect of C_{55} is on the high-frequency limit of the S_0 and A_0 modes [27].

NONMOVING PAPER RESULTS USING THE TWM METHOD

Figures 6(a) and (b) show examples of recorded signals obtained on nonmoving copy paper using the TWM setup in MD and CD. The signals were recorded at generation-detection distances of 10 and 15 mm for Fig. 6(a) and 10 and 20 mm for Fig. 6(b). One important achievement of the detection method is the quality of single-shot signals without any averaging. The presence of the symmetric S_0 mode wave is observed first. It is followed by the antisymmetric A_0 mode wave. As expected, this signal is significantly larger in amplitude and duration than the S_0 signal. Also, it is dispersive and has lower frequency content. These are all characteristics of a bending wave. Also, saturation of the A_0 signal in Fig. 6(a) at 10 mm was due to generation in the ablation regime overloading the photodiode, and this resulted in the beating of this signal.

To determine the phase velocity of the S_0 mode from Fig. 6(a), the cross-correlation function of the two S_0 signals was obtained. This is shown in Fig. 7. It indicates that there is a maximum peak at 1.72 μs. Since this peak exists at the relative time delay between the two signals, the resulting S_0 velocity can be found by dividing it by the relative distance between the two detection points, i.e. 5 mm. The resulting velocity is 2907 ± 29 m/s for this particular case. In comparison, the S_0 velocity obtained by the contact method was 3274 ± 33 m/s. The difference may be explained by the fact that the S_0 mode is very sensitive to the exact measurement of the generation-detection distance and the local characteristics of the paper surface where the laser beam is shot. Hence, several measurements must be made to be statistically valid. More statistically valid

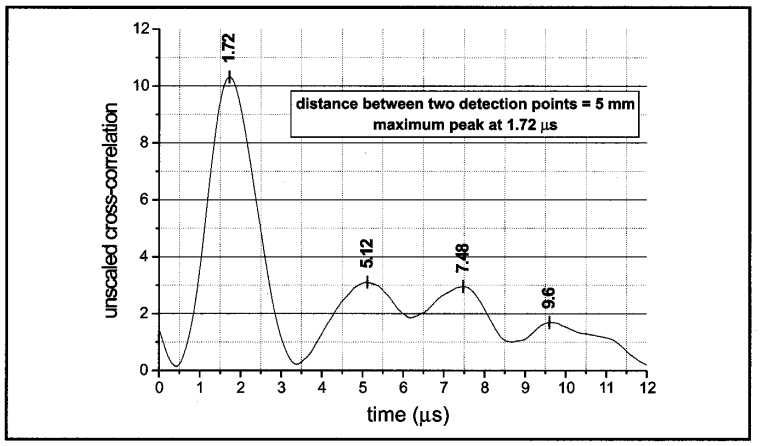

Fig. 7. Cross-correlation of two S_0 signals in Fig. 6(a).

measurements of the S_0 velocity were performed previously [29,36], which showed that the contact and noncontact methods provided similar values.

The S_0 mode velocity measurements in the low-frequency region can be used to determine the elastic stiffness constants, Q_{11} in MD and Q_{22} in CD [18]. As previously indicated, the S_0 mode also contains information on C_{33} (ZD). Ideally, if the S_0 mode can be measured accurately around the cut-off frequency, C_{33} can be determined. Yet, the nature of the narrow-frequency bandwidth of the S_0 mode makes it difficult to estimate C_{33} using this method [27]. Further work is needed to evaluate C_{33} from the S_0 mode, especially with thick linerboard samples in which the S_0 mode cut-off frequency is known to be in a lower frequency region when compared to thinner papers such as copy paper.

The technique used here to extract information from the A_0 mode is based on the method originally suggested by Sachse and Pao [37]. Later, Schumacher et al. [35] applied it to Lamb waves. In this method, the phase velocity is extracted from the frequency domain information and unwrapped as a function of frequency. Referring to Fig. 6(b), only the signal region corresponding to the A_0 mode is selected and the rest is zero-padded. Each signal is windowed using a rectangular window and processed in the frequency domain. The phase angle spectra are unwrapped and their difference, $\Delta\phi(f)$, is directly related to the phase velocity of the A_0 mode using the following relationship:

$$c(f) = \frac{-2\pi \cdot f \cdot \Delta d}{(\Delta\phi(f) + 2m\pi)} \qquad (1)$$

where $c(f)$ is the phase velocity of the A_0 mode (m/s), f is the frequency (Hz), Δd is the distance between two detection points (m), $\Delta\phi(f)$ is in radians, and m is an integer for the correction of the phase at low frequency.

Figure 8 shows the combination of the steps described above for evaluating the A_0 mode wave using signals recorded in Fig. 6(b). The amplitude spectra indicate that significant signal energy exists only in the frequency region between 0.005 and 0.3 MHz. This trend is consistent throughout the trials. On the other hand, the results given by Johnson [27] on nonmoving copy paper using a Mach-Zehnder interferometer showed that energy was present up to 1.0 MHz. The reason for not being able to detect higher frequency A_0 information with the TWM configuration is unclear. It may be related to the generation method.

Of importance is the integer m to be used in Eq. (1) to correct the phase angle in the very low frequency region (<5 kHz) where the signal energy is also low. As the phase unwrapping is performed from low to high frequencies, the accuracy of the phase measurement at a given frequency depends upon the phase values at lower frequencies. A small error in phase angle at very low frequencies will accumulate and produce significant differences at higher frequencies.

Figure 9 shows a comparison between the theoretical A_0 dispersion curve and the results with corrected phase angles. The theoretical curve was obtained from the numerical solution of A_0 mode dispersion equation for a given range of frequency. The valid range covers the frequency region where the signal energy is present. The phase velocity determined from the original phase difference tends to predict a higher magnitude in the low-frequency region below 0.1 MHz, while the one corrected with -2π seems to match the theoretical curve in the low-frequency region. Comparison with other paper samples shows that good prediction seems to come from the correction of -2π or -4π. Nevertheless, further analysis is underway to determine the accuracy of the correction term m for the A_0 mode analysis [36].

Figure 10 shows a series of signals obtained on copy paper in CD using the Photo-EMF setup at web speeds up to 25 m/s. The distance between generation

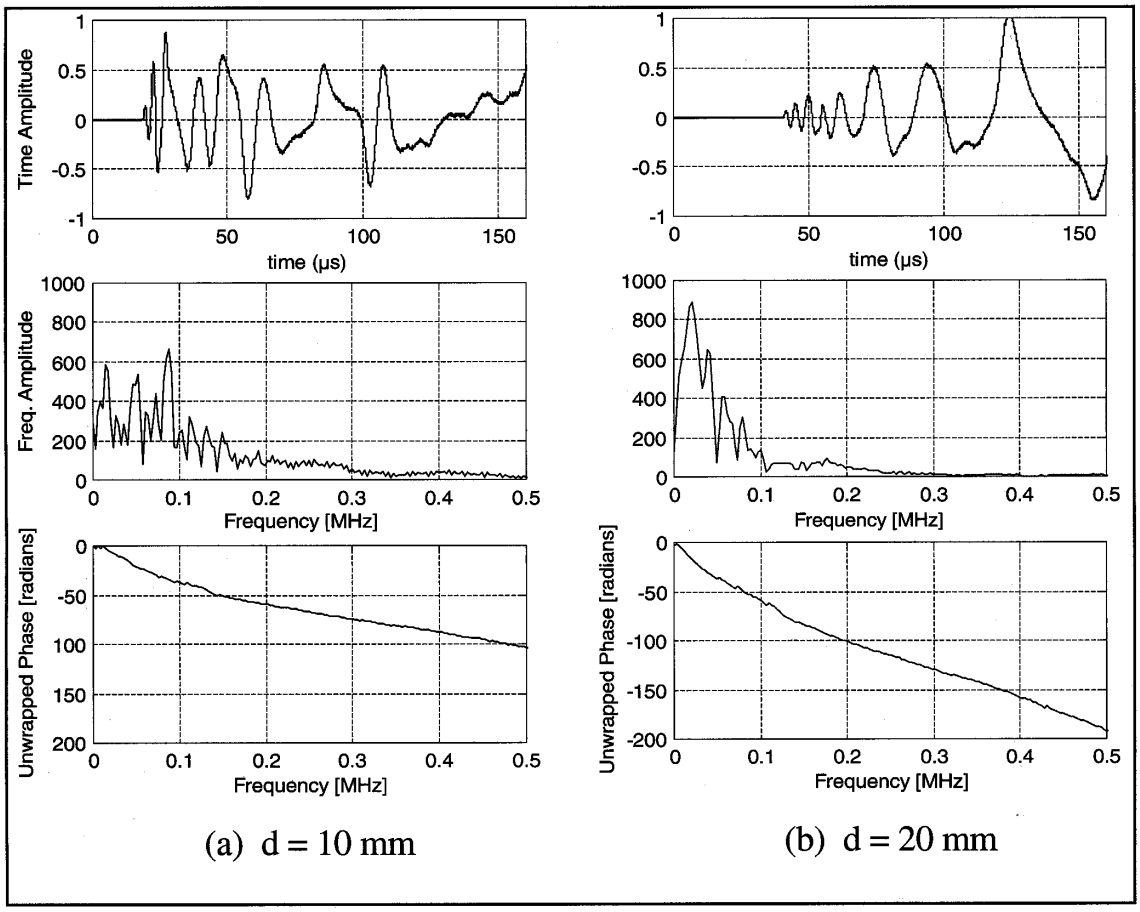

Fig. 8. A_0 mode analysis of signals on static copy paper in CD; top: zero-padded A_0 signal in time domain, middle: amplitude spectrum, bottom: unwrapped phase angle spectrum.

and detection points, power of the detection laser, and energy per pulse of the generation laser were maintained at 10 mm, 1.33 W, and 25.6 mJ, respectively. Single-shot results are reported up to 6 m/s. While the S_0 mode signal is easily observed only up to 6 m/s, the A_0 mode is detected up to 25 m/s, e.g. above the production speed for copy paper. By improving the current experimental configuration and optimizing the laser optics, the S/N ratio can be further improved. Results were also obtained on moving 42 lb linerboard samples. Figure 11 shows averaged signals in MD at web speeds up to 20 m/s, e.g. above the production speed for linerboard. The distance between generation and detection points was 10 mm. While the A_0 mode is detected clearly up to 20 m/s, the S_0 mode is barely observed at even the lowest speed.

To analyze the effect of the generation-detection separation distance on moving paper results, copy paper measurements were made at 10, 15 and 20 mm separation distances. Results obtained at web speeds of 2 and 10 m/s are shown in Figs. 12(a) and (b), respectively. S_0 signals were not detected at 10 m/s. The dispersive nature of the A_0 mode is clearly seen.

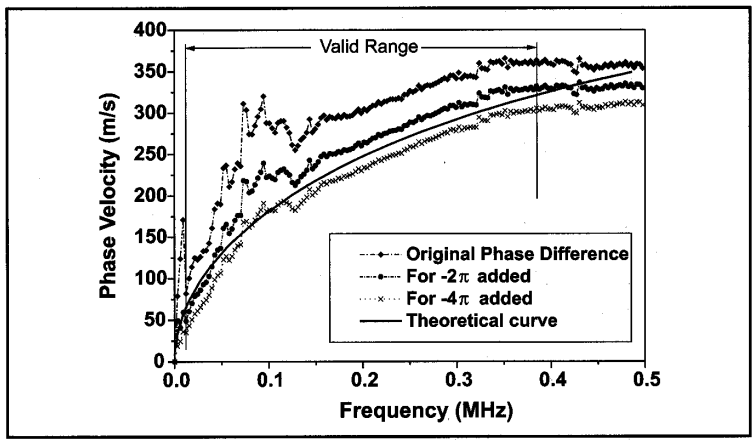

Fig. 9. A_0 mode phase velocities computed using Eq. (1) for different values of m (0,-1,-2) for phase correction.

It is interesting to observe attenuation and dispersion of Lamb waves in amplitude and wave speed. As the generation/detection

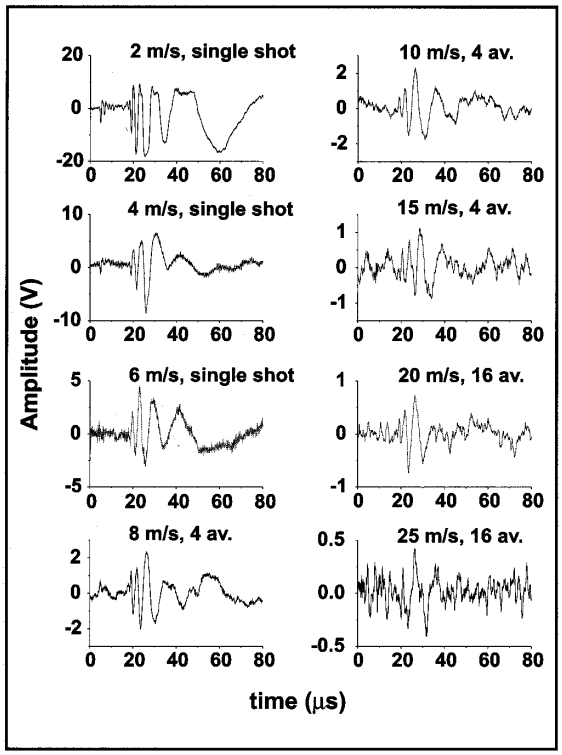

Fig. 10. Signals on moving copy paper in CD.

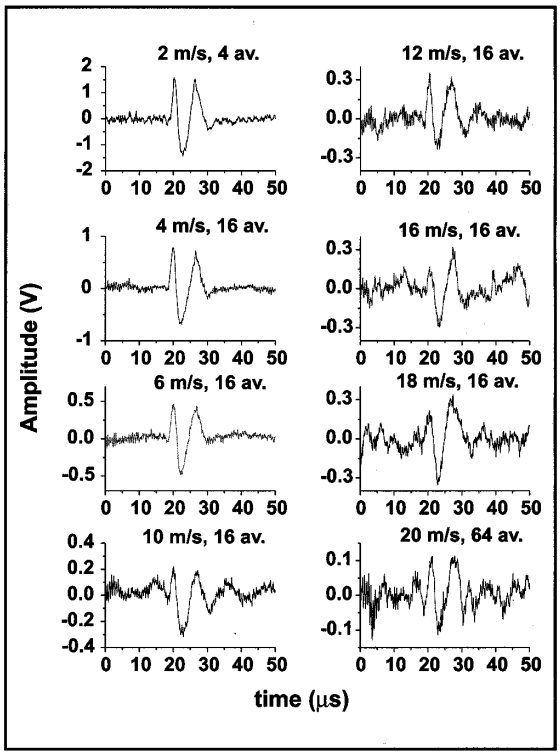

Fig. 11. Signals on moving 42 lb linerboard in MD.

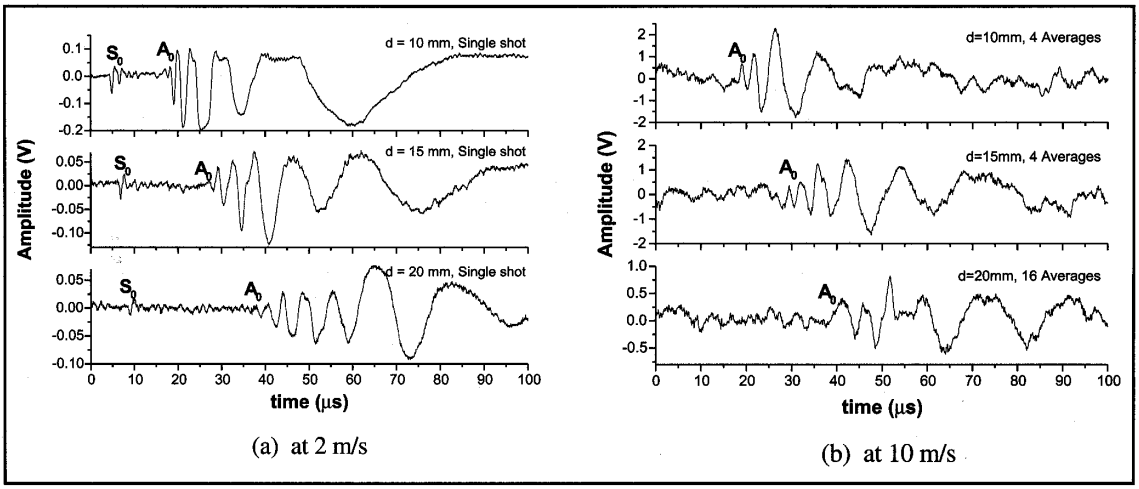

Fig. 12. Comparison of Lamb waves for different generation-detection separation distances in copy paper in CD at 2 and 10 m/s.

distance increased, the amplitudes of S_0 and A_0 signals decreased. It is shown that the high-frequency A_0 waves were attenuated in travelling the extra distance. On the other hand, the S_0 wave maintained almost the same arrival time, which indicates no dispersion in S_0 wave speed although the signal attenuation took place in amplitude.

Figure 13 shows the A_0 mode analysis at 10 and 20 mm separation distances. The zero-padded A_0 signals are shown and the energy of the signals is mostly present below 0.4 MHz (see amplitude spectra). Figure 14(a) shows the comparison of the original and several phase-corrected A_0 mode phase velocities shown against a theoretical curve and an approximate curve. The approximate curve was obtained by simplifying the theoretical dispersion equation applicable for a low-frequency region [18,38]. Figure 14(b) shows the same A_0 mode results in a different format, making it easier to interpret. The A_0 phase velocity is divided by the square root of the corre-

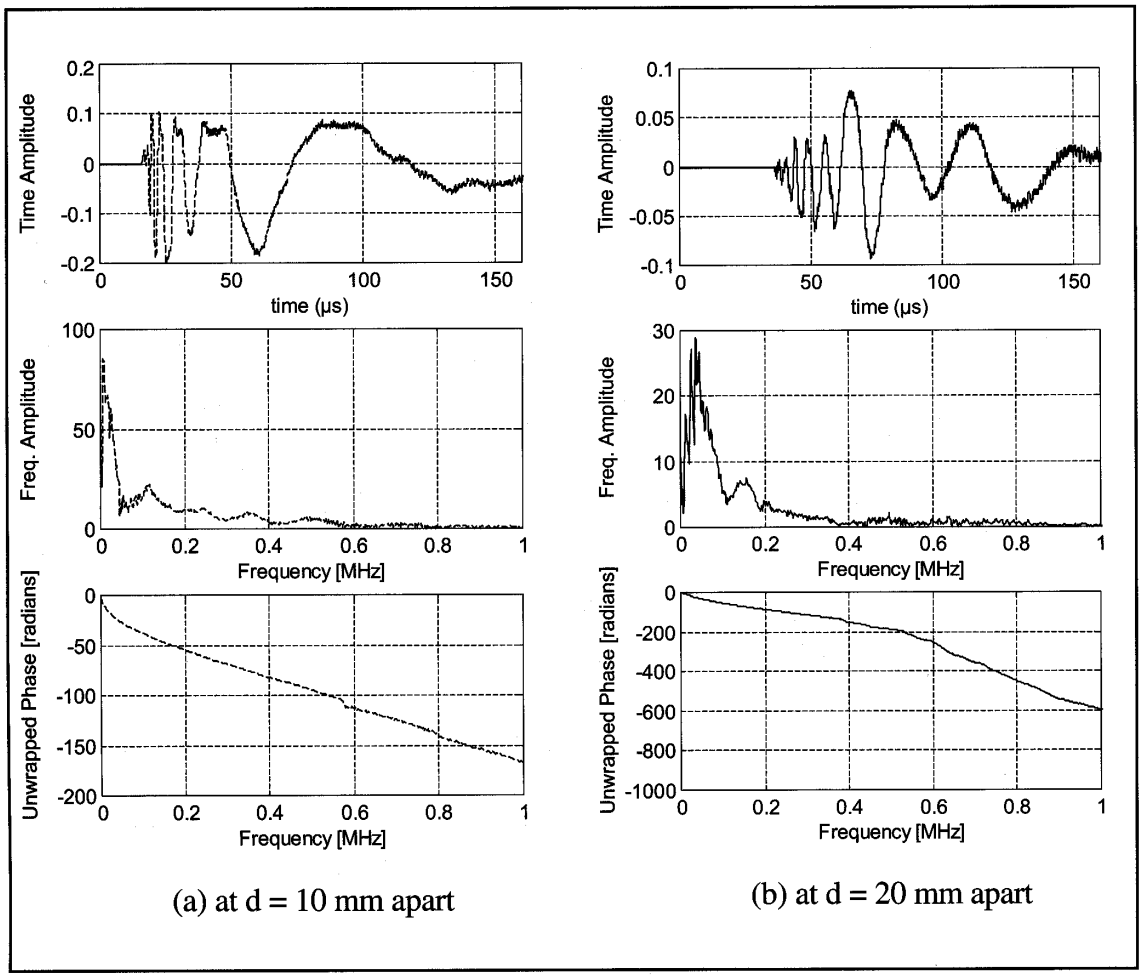

Fig. 13. A_0 mode analysis at 10 and 20 mm distances between generation and detection in copy paper in CD at 2 m/s.

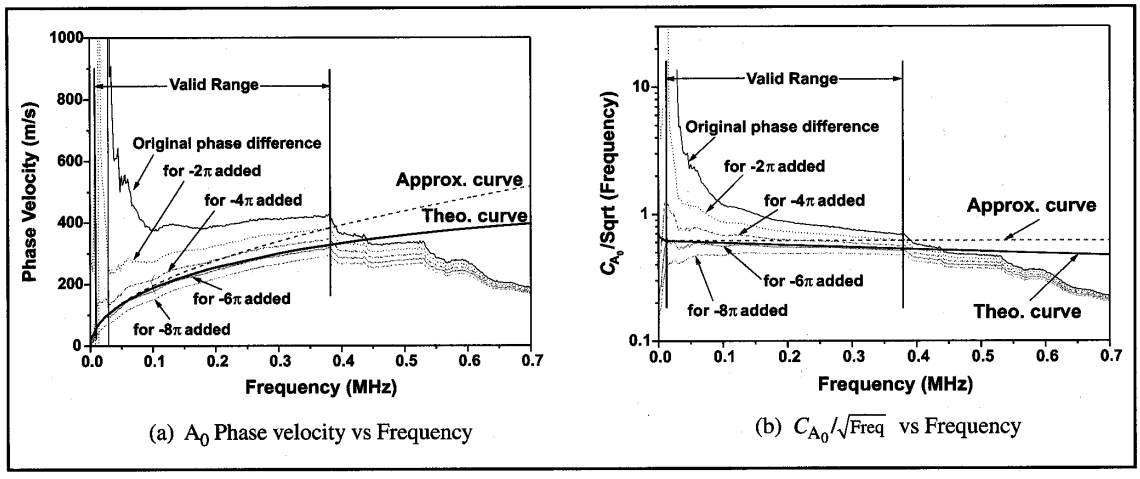

Fig. 14. Comparison of data analysis from Fig. 13 for C_{A_0}, and $C_{A_0}/\sqrt{Freq}$ as a function of frequency, where C_{A_0} is A_0 phase velocity.

sponding frequency so that the approximation curve becomes linear. The theoretical dispersion curve becomes a decreasing line that deviates away from the approximate curve. It is also easier to compare each phase correction with the approximate and theoretical curves. Eventually, the bending stiffness of paper may be obtained from Fig. 14(b) since the bending stiffness is a function of basis weight and the fourth power of $C_{A_0}/\sqrt{\text{Freq}}$. It may also be possible to obtain information related to the out-of-plane shear, C_{44} and C_{55}, from the data. Nevertheless, further work is required to extract bending stiffness and out-of-plane shear information.

FUTURE DIRECTION AND POTENTIAL OF THE TECHNOLOGY

The development of on-machine paper stiffness sensors has been an on-going process for over two decades because mechanical properties are critical to the papermaking process, converting operations, and end-use performance. Until now, most of the research has focused on the development of contact methods, and some of these methods have started to appear in commercial applications [39]. Nevertheless, noncontact concepts are far more desirable to the papermaker. Also, it is hypothesized that the availability of a noncontact method would simplify the development of full-sheet inspection systems for paper stiffness. Based on current knowledge and preliminary results of noncontact laser ultrasonics, the method has the full potential to become a next generation application to measure on-line paper stiffness properties. Its deployment is challenging, but it should provide the necessary information to fulfill the needs of elaborate papermaking control strategies. Further work needs to be pursued to address the inverse analysis of paper stiffness properties based on Lamb waves as well as the bending stiffness and the shear rigidity properties of a wide range of papers.

CONCLUSIONS

This study investigated the use of noncontact laser ultrasonics to measure paper stiffness on nonmoving and moving paper. The TWM method was used to detect signals on nonmoving paper. The S_0 mode was analyzed using a cross-correlation method, and the current status of the A_0 mode analysis technique was discussed. The Photo-EMF method was found useful to detect Lamb waves in MD and CD on moving paper at production speeds, but left minor visible marks on the paper surface when ablation was used. This is not acceptable to paper manufacturers and current efforts are aimed at improving generation efficiency and detection sensitivity so that a good signal-to-noise ratio can be achieved without leaving a visible mark on the paper. The S_0 and A_0 wave results were evaluated to investigate the performance of the noncontact method compared to the contact method. The attenuation of the A_0 wave was addressed. The effect of different generation/detection distances was presented based upon A_0 mode analysis. Future directions and the potential of noncontact technology for on-line application were briefly commented upon.

ACKNOWLEDGEMENTS

The authors would like to thank C.C. Habeger from IPST, K. Telschow and V. Deason from Idaho National Engineering and Environmental Lab, and B. Pouet and M. Klein from Lasson Technologies. Support for the project was provided by the Member Companies of IPST. The authors also wish to thank for their collaborative work on this project the U.S. Department of Energy, Office of Industrial Technologies for its support through the Agenda 2020 Program for the Pulp and Paper Industry [Cooperative Agreement No. DE-FC07-97ID13578].

REFERENCES

1. BAUM, G.A., "Elastic Properties, Paper Quality, and Process Control", *Appita* 40(4):288–293 (1987).
2. PAPADAKIS, E.P., "Ultrasonic Methods for Modulus Measurement in Paper", *Tappi J.* 56(2):74–77 (1973).
3. LU, M.T., "On-Line Measurement of Strength Characteristics of a Moving Sheet", *Tappi J.* 58(6):80–81 (1975).
4. BAUM, G.A. and HABEGER, C.C., "On-Line Measurements of Paper Mechanical Properties", *Tappi J.* 63(7):63–66 (1980).
5. BAUM, G.A. and HABEGER, C.C., "On-Line Ultrasonic Velocity Gauge", U.S. Patent 4,291,577 (issued in Sept. 1981).
6. KAZYS, K.R., "Ultrasonic Methods for Non-Destructive Testing of Paper", Proc. XXth Intl. Conf. Acoustics and Ultrasound, Prague, 192–193 (1981).
7. SENKO, E. and THORPE, J., "On-Line Ultrasonic Measurement of Sheet Modulus", *Tappi J.* 68(2):95–99 (1985).
8. HABEGER, C.C. and BAUM, G.A., "On-Line Measurement of Paper Mechanical Properties", *Tappi J.* 69(6):106–111 (1986).
9. VAHEY, D.W., "An Ultrasonic-Based Strength Sensor for On-Line Measurements", *Tappi J.* 70(3):79–82 (1987).
10. ORKOSALO, J.J., "System and Process for Measuring Ultrasonic Velocity", U.S. Patent 4,688,423 (issued in Aug. 1987).
11. VAHEY, D.W., "Correlating the On-Line Measurement of Ultrasonic Velocity with Strength Properties", *Tappi J.* 71(4):149–152 (1988).
12. CHASE, L., GOSS, J. and ANDERSON, L., "On-Line Sensor for Measuring Strength Properties", *Tappi J.* 72(12):89–97 (1989).
13. BRODEUR, P.H., HALL, M.S. and ESWORTHY, C., "Sound Dispersion and Attenuation in the Thickness Direction of Paper Materials", *J. Acoust. Soc. Am.* 94(4):2215–2225 (1993).
14. BRODEUR, P.H., "Out-of-Plane Ultrasonic Testing of Paper Materials Using Fluid-filled Rubber Wheels", *Tappi J.* 77(3):213–218 (1994).
15. CRESSON, T.M., GOSS, J.D. and WALLACE, B.W., "Sensor, System and Method for Determining Z-Directional Properties of a Sheet", U.S. Patent 5,297,062 (issued in March 1994).
16. WILLIAMS, P. and PANKONIN, B.M., "On-Line Measurement of Ultrasonic Velocities in Wet Manufacturing Processes", U.S. Patent 5,398,538 (issued in March 1995).
17. LUUKKALA, M., HEIKILA, P. and SURAKKA, J., "Plate Wave Resonance, A Contactless Test Method", *Ultrasonics* 9:201–208 (1971).
18. HABEGER, C.C., MANN, R.W. and BAUM, G.A., "Ultrasonic Plate Wave in Paper", *Ultrasonics* 17:57–62 (1979).
19. LEUGERS, M.A., "Laser Induced Acoustic Generation for Sonic Modulus", U.S. Patent 4,622,853 (1986).
20. PACE, S.A. and SALAMA, S.S., "Laser Induced Acoustic Generation for Sonic Modulus", U.S. Patent 4,674,332 (1987).
21. KEYES, M.A. and THOMPSON, W.L., "Non-Contacting On-Line Paper Strength Measuring System", U.S. Patent 5,025,665 (1991).
22. HUTCHINS, D.A., SCHINDEL, D.W., BASHFORD, A.G. and WRIGHT, W.M.D., "Advances in Ultrasonic Electrostatic Transduction", *Ultrasonics* 36(1–5):1–6 (1998).
23. SCHINDEL, D.W. and HUTCHINS, D.A., "Applications of Micromachined Capacitance Transducers in Air-Coupled Ultrasonics and Nondestructive Evaluation", IEEE Trans. Ultrason. Ferroelec. Freq. Cont., 42(1):51–58 (1995).
24. SCRUBY, C.B. and DRAIN, L., Laser Ultrasonics – Techniques and Applications, Adam Hilger-IOP Publishing, Bristol (1990).
25. MONCHALIN, J.P., AUSSEL, J.-D., HEON, R., KEN, C.K., BOUDREAULT, A. and BERNIER, R., "Measurement of In-Plane and Out-of-Plane Ultrasonic Displacements by Optical Heterodyne Interferometry," *J. Nondestr. Eval.* 8(2):121–133 (1989).
26. BRODEUR, P.H., BERTHELOT, Y.H., JOHNSON, M.A. and GERHARDSTEIN, J.P., "Paper Stiffness Monitoring Using Laser Ultrasonics," Proc. 1996 IEEE Intl. Ultrasonics Symp., San Antonio (Nov. 3–6, 1996).
27. JOHNSON, M.A., "Investigation of the Mechanical Properties of Copy Paper Using Laser Generated and Detected Lamb Waves", Ph.D. Thesis, Georgia Inst. Tech. (1996).
28. JOHNSON, M.A., BERTHELOT, Y.H., BRODEUR, P.H. and JACOBS, L.A., "Investigation of Laser Generation of Lamb Waves in Copy Paper", *Ultrasonics* 34(7): 703–710 (1996).
29. BRODEUR, P.H., JOHNSON, M.A., BERTHELOT, Y.H. and GERHARDSTEIN, J.P., "Noncontact Laser Generation and Detection of Lamb Waves in Paper", *J. Pulp Paper Sci.* 23(5):J238–J243 (1997).
30. LAFOND, E., GERHARDSTEIN, J. and BRODEUR, P., "Non-Contact Characterization of Static Paper Materials Using a Photorefractive Interferometer", Proc. SPIE Conf. Process Control and Sensors for Manufacturing, Newport, CA, SPIE3589:30–41 (1999).
31. POUET, B., LAFOND, E., PUFAHL, B., BACHER, D., BRODEUR, P. and KLEIN, M., "On-Machine Characterization of Moving Paper Using a Photo-EMF Laser Ultrasonics Method", Proc. SPIE Conf. Process Control Sensors for Manufacturing, Newport, CA, SPIE3589:160–169 (1999).
32. VIKTOROV, I.A., "Rayleigh and Lamb Waves", Plenum Press, N.Y. (1967).

33. HABEGER, C.C., VAN ZUMMEREN, M.L., WINK, W.A., PANKONIN, B.M. and GOODLIN, R.S., "Using a Robot-Based Instrument to Measure the In-Plane Ultrasonic Velocities of Paper," *Tappi J.* 72(7):171–175, (1989).
34. HABERGER, C.C. and WINK, W.A., "Ultrasonic Velocity Measurements in the Thickness Direction of Paper", *J. Appl. Polymer Sci.* 32:4503–4540 (1986).
35. SCHUMACHER, N.A., BURGER, C.P. and GIEN, P.H., "A Laser-Based Investigation of High-Order Modes in Transient Lamb Waves", *J. Acoust. Soc. Am.* 93(5):2981–2984 (1993).
36. JONG, J.H., BRODEUR, P.H. and GERHARDSTEIN, J.P., "Measurement and Analysis of Stiffness Properties in Moving Paper Using Noncontact Laser Ultrasonics", Proc. Intl. Paper Physics Conf., San Diego, 19–27 (1999).
37. SACHSE, W. and PAO, Y.H., "On the Determination of Phase and Group Velocities of Dispersive Waves", *J. Appl. Phys.* 49(8): 4320–4327 (1978).
38. MANN, R.W., BAUM, G.A. and HABEGER, C.C., "Determination of All Nine Orthotropic Elastic Constants for Machine Made Paper", *Tappi J.* 63(2):164–167 (1980).
39. KOPKIN, B., "On-Line Measurement of Strength and Elastic Properties of a Running Paper Web", *Tappi J.* 82(5):137–140 (1999).

REFERENCE: JONG, J.H., BRODEUR, P.H., LAFOND, E.F., GERHARDSTEIN, J.P. and PUFAHL, B.M., Laser Ultrasonics for Noncontact Measurement of Lamb Waves in Static and Moving Paper. Journal of Pulp and Paper Science. 26(10):358–366 October 2000. Paper presented at the 85th Annual Meeting of the Pulp and Paper Technical Association of Canada, held in Montreal, QC, January 26–29, 1999. Not to be reproduced without permission from the Pulp and Paper Technical Association of Canada. Manuscript received November 13, 1998; revised manuscript approved for publication by the Review Panel June 8, 2000.

KEYWORDS: MEASURING INSTRUMENTS, LASERS, ULTRASONIC FREQUENCIES, MONITORING, STIFFNESS TESTERS, PROCESS CONTROL, STIFFNESS, MECHANICAL PROPERTIES.

MICROGRAPHS WANTED!

Do you have any interesting micrographs which would be suitable for publication on the front covers of the ***Journal of Pulp and Paper Science***? Preference is given to micrographs with esthetic appeal; if they are scientifically informative, that is a bonus.

Coloured micrographs would be preferred, but black and white ones which could be printed with a coloured tint would also be considered. The micrographs should be printed on glossy paper 4" x 4" square (or slightly larger). The field should contain no μ-marks, dates, information, arrows, etc. Each micrograph should be submitted with a caption, including magnification, and your name, company affiliation and address. This information will appear on the inside front cover of the issue in which the microphotograph is published.

We can also accept micrographs which have been scanned at high resolution (X1200 dpi). These should be submitted on a 100 MB Zip disk, which will be returned promptly.

Microphotographs and/or Zip disks should be sent to:

Dr. Derek Page
Scientific Editor, Journal of Pulp and Paper Science
c/o Paprican, 570 St. John's Blvd.
Pointe Claire, QC, Canada H9R 3J9
Tel: (514) 630-4100; Fax: (514) 630-6971
e-mail: dpage@paprican.ca